VIP

Synthesis and Supramolecular Properties of Molecular Clips with Anthracene Sidewalls

Frank-Gerrit Klärner,*[a] Björn Kahlert,[a] Roland Boese,[b] Dieter Bläser,[b] Alberto Juris,[c] and Filippo Marchioni[c]

Abstract: Novel molecular clips with anthracene sidewalls (**1a–c**) were synthesized; they form stable host–guest complexes with a variety of electron-deficient aromatic and quinoid molecules. According to single-crystal structure analyses of clip **1c** and 1,2,4,5-tetracyanobenzene (TCNB) complex **14@1b**, the clips' anthracene sidewalls have to be compressed substantially during the complex formation to provide attractive π–π interactions between the aromatic guest molecule and the two anthracene sidewalls in the complex. The compression and expansion of aromatic sidewalls are calculated by molecular mechanics to be low-energy processes, so the energy required for compression of the anthracene sidewalls during complex formation is apparently overcompensated by the gain in energy resulting from the attractive π–π interactions. The finding that complexes of the clips **1a–c** are more stable than those of the corresponding clips **2a–c** can be explained in terms of the larger van der Waals contact surfaces of the anthracene sidewalls in **1a–c** (relative to the naphthalene sidewalls in **2a–c**). Color changes resulting from charge-transfer (CT) bands are observed in complex formation by **1a–c**: from colorless to red or purple with TCNB (**14**), and from yellow to green with 2,4,7-trinitro-9-fluorenone TNF (**17**). Independently, the host **1b** and guest **14** fluoresce from their respective excited singlet states, whilst in the complex **14@1b** the charge-transfer state quenches the higher-energy singlet states of the two components, and as a result luminescence is only observed from this new CT state. To the best of our knowledge, complex **14@1b** is the first example of CT luminescence from a host–guest complex. The binding constant determined for the formation of the TCNB complex **14@1b** from a UV/Vis titration experiment (K_a = 12400 M^{-1}) agrees well with the value (K_a = 12800 M^{-1}) obtained by ^1H NMR titration.

Keywords: binding constants · host–guest complexes · luminescence · molecular clips and tweezers · supramolecular chemistry

Introduction

Efficient synthetic receptors with the capability for selective substrate binding are important for understanding of molecular recognition in chemical and biological systems.[1–4] We have recently described the syntheses and some supramolecular properties of benzene- and/or naphthalene-spaced receptors of types **2**,[5] **3**,[6] and **4**.[7–11] The dimethylene- and trimethylene-bridged compounds **2** and **3** were called molecular clips, because they form complexes by "clipping" an aromatic substrate inside the receptor cavity, with its plane of molecule almost parallel to the naphthalene side walls. The tetramethylene-bridged compounds of type **4** have been named molecular tweezers, because the substrates are usually taken up through the receptor tips (made by the terminal benzene rings), similarly to the working principle of mechanical tweezers, and are moved inside the receptor cavity to a position in which the plane of molecule is arranged nearly parallel to the central naphthalene spacer unit of **4**.[12] All three types of receptors selectively bind electron-deficient aromatic neutral and cationic substrates by multiple attractive noncovalent CH–π and π–π interactions. Electron-

[a] Prof. Dr. F.-G. Klärner, B. Kahlert
Institut für Organische Chemie der Universität Duisburg-Essen
45117 Essen (Germany)
Fax: (+49) 201-183-4252
E-mail: frank.klaerner@uni-essen.de

[b] Prof. Dr. R. Boese, D. Bläser
Institut für Anorganische Chemie der Universität Duisburg-Essen
45117 Essen (Germany)

[c] Prof. Dr. A. Juris, Dr. F. Marchioni
Dipartimento di Chimica "G. Ciamician" Università di Bologna via Selmi 2
40126 Bologna (Italy)

Supporting information for this article is available on the WWW under http://www.chemeurj.org/ or from the author.

 DOI: 10.1002/chem.200401257

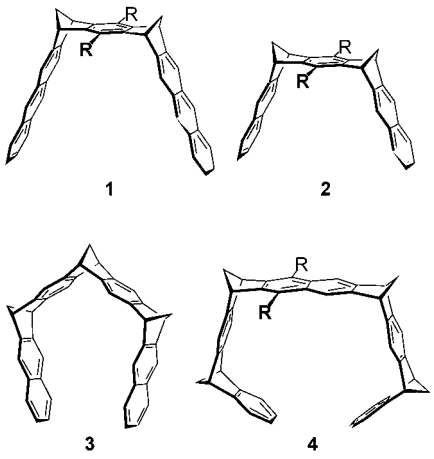

a: R = OAc, **b**: R = OH, **c**: R = OMe

rich arenes or anions are not complexed by these receptors within the limits of experimental detection. This high selectivity toward electron-deficient substrates was correlated with markedly negative electrostatic potential surfaces (EPSs) calculated for the concave faces of **2**–**4** by quantum-chemical methods.[13,14] When analogous calculations were performed for the substrates binding to **2**–**4** the complementary nature of their EPSs became evident, suggesting that the substrate–receptor binding in these complexes is predominantly electrostatic in nature. The complexes of dimethylene-bridged clips of type **2** with many substrates, however, turned out to be less stable than the corresponding ones of the tri- and tetramethylene-bridged receptors **3** or **4**.[15] There are two possible explanations for this finding: according to single-crystal structure analyses of, for example, the complex between 1,2,4,5-tetracyanobenzene (TCNB; **14**) and clip **2b**,[5] 1) the van der Waals contact surfaces of the naphthalene side walls of **2b** are relatively small to embrace the substrate molecule completely, and 2) the naphthalene side walls of **2b** have to be compressed so that both naphthalene units can enter into attractive π–π interactions with the substrate molecule. To improve the properties of the dimethylene-bridged receptors it was of great interest to increase the van der Waals contact surfaces of the aromatic sidewalls. Here we report the synthesis and supramolecular properties of the dimethylene-bridged clips **1a–c** with anthracene side walls. Since anthracenes usually show strong fluorescence these clips are also of further interest as potential chemical sensors for various substances.

Results and Discussion

Synthesis of the dimethylene-bridged anthracene clips 1a-c: We first tried to prepare **1a** by starting from 2,3-bis(dibromomethyl)naphthalene (**5**)[16,17] and bisdienophile **8a**[18] as building blocks, analogously to the successful synthesis of the corresponding naphthalene clips **2a–c**.[5] The one-pot reactions shown in Scheme 1, however, do not lead to clip **1a**. The observation of dibromonaphthocyclobutene **7** as final product suggests that the 1,4-Br_2 elimination of **5** on treatment with NaI does indeed proceed to generate *o*-naphthoquinodimethane **6** as a reactive intermediate, but that this undergoes monomolecular electrocyclic ring closure to **7** more rapidly than it does the desired bimolecular Diels–Alder cycloaddition to bisdienophile **8a**. Since the aromaticity of both rings has to be given up in *o*-naphthoquinodimethane (**6**), this intermediate is certainly less stable, and

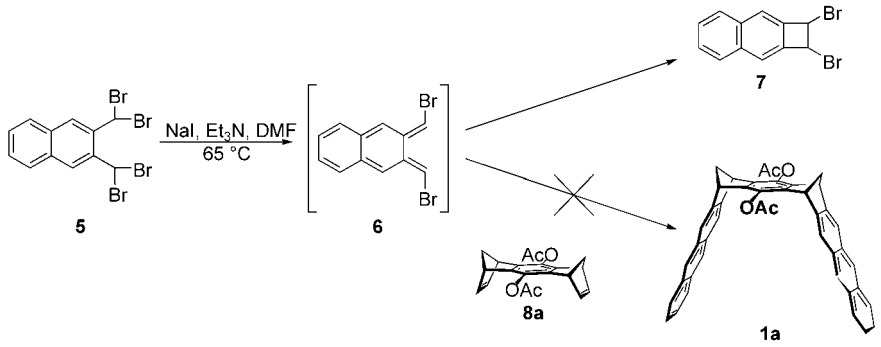

Scheme 1. Attempts to synthesize the benzene-anthracene clip **1a** by the *o*-naphthoquinodimethane route.

hence more reactive, than the corresponding *o*-quinodimethane derivative (generated from bis(dibromomethyl)benzene under similar conditions).[19–21] Evidently the bimolecular Diels–Alder reaction (which is limited in its rate by diffusion) cannot compete with the intramolecular electrocyclization in the case of **6**.

The anthracene clips **1a–c** could be prepared in four to six steps as shown in Scheme 2. The tetrabromo-*o*-quinodimethane **10** (generated by 1,4-Br_2 elimination from hexabromo-*o*-xylene **9**)[22] reacted with bisdienophile **8a**[18] to afford the Diels–Alder bisadduct **11a**, which spontaneously eliminated HBr under the reaction conditions, producing the tetrabromodiacetoxy-substituted naphthalene clip **12a**. The acetoxy groups in **12a** were converted into methoxy groups by basic ester hydrolysis and subsequent methylation without isolation of the intermediately formed hydroquinone **12b**. The dimethoxy-substituted clip **12c** could also be directly prepared in 34% yield by starting from hexabromo-*o*-xylene **9** and bisdienophile **8c**. In this case, however, the isolation of pure **12c** from the reaction mixture by LC separation turned out to be more difficult than in the case of **12a**, so we prefer to prepare **12c** via **12a**. Debromination of **12c** with *n*-butyllithium produced a formal bisaryne that was

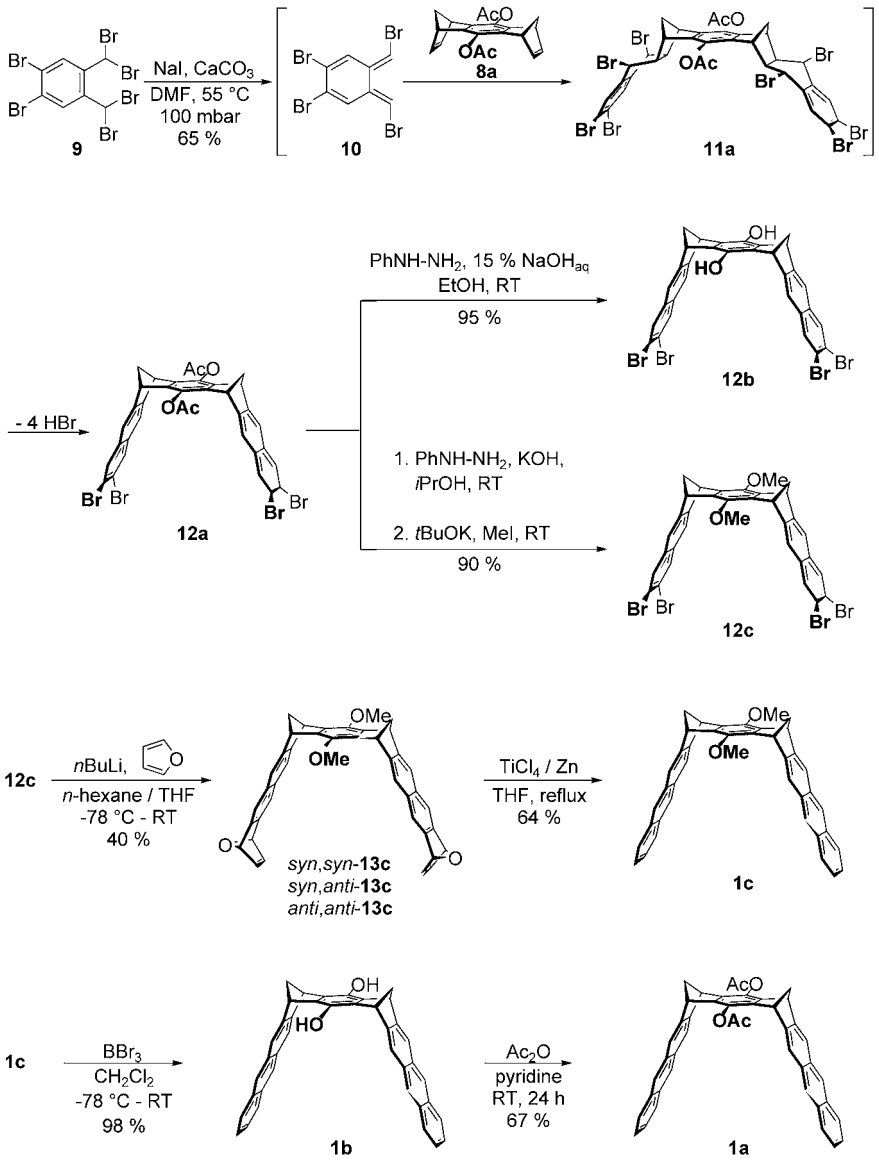

Scheme 2. The synthesis of the benzene-spaced anthracene clips **1a–c** by the *o*-tetrabromoquinodimethane route.

trapped through a Diels–Alder reaction with furan to afford a mixture of all three diastereomeric bisadducts *syn*,*syn*-**13c**, *syn*,*anti*-**13c**, and *anti*,*anti*-**13c**. The desired clip **1c** could be obtained from this mixture of bisadducts without separation by deoxygenation with low-valent titanium generated in situ from titanium tetrachloride and zinc powder.[23] The dimethoxy-substituted clip **1c** could be converted into the hydroquinone clip **1b** by treatment with borane tribromide[24] and **1b** into the diacetoxy-substituted derivative **1a** by esterification of **1b** with acetic anhydride.

The bowl-shaped structures of **1a–c** were unambiguously determined by single-crystal structure analysis of **1c** (the precursor of **1a** and **1b**: Figure 1) and the spectral data (see Experimental Section).

According to the site symmetry *a* (*mm*) of the *Fmm*2 space group, the molecules of **1c** possess $C2_v$ symmetry with one mirror plane perpendicular to the anthracene moieties and one to the central benzene ring, intercepting the methoxy oxygen and carbon atoms. Thus, the molecules are lined up along the *a* axis of the cell like clips on a clothesline, with the methoxy groups pointing towards each other at distances of 2.2 Å for the methoxy hydrogen atoms. The methoxy group hydrogen atoms approach each other by 0.8 Å, so they have to adopt alternating up-down positions to avoid clashes with the neighboring groups, which results in a 50% positional disorder. The neighboring methoxy groups are mutually embraced by further, parallel positioned clips. The interplanar angle between the mean planes of the anthracene moieties (max deviation 0.014 Å) is 65.1° and the distance between the atoms C10 to the symmetry equivalent on the other side of the clip is 14.5 Å.

The dimethylene-bridged anthracene clips 1a–c as synthetic receptors and comparison with the corresponding naphthalene clips 2a–c: The magnetic anisotropy of the receptor arene units makes ^{1}H NMR spectroscopy a very sensitive probe for examining the complexation of a substrate molecule inside the cavity of one of the receptor molecules **1a–c** or **2a–c**. The complex formation can be easily detected by pronounced upfield shifts of the signals in the ^{1}H NMR spectrum of the substrate after addition of the receptor. In all complexations reported here the receptor–substrate association and dissociation are fast processes with respect to the NMR timescale. Thus, the maximum complexation-induced ^{1}H NMR shifts ($\Delta\delta_{max}$) of the substrate signals ($\Delta\delta_{max} = \delta_0 - \delta_C$; δ_0 and δ_C are the ^{1}H NMR shifts of the free and the complexed substrate, respectively), the association constants (K_a), and the free enthalpies of association (ΔG) could be determined by ^{1}H NMR titration experiments from measurements of the dependence of the complexation-induced ^{1}H NMR shifts ($\Delta\delta_{obs}$) of the substrate signals on the receptor concentration ($[R]_0$) at constant substrate concentration ($[S]_0$ = const.) as described in the Experimental Section ($\Delta\delta_{obs} = \delta_0 - \delta_{obs}$; δ_{obs} is the substrate ^{1}H

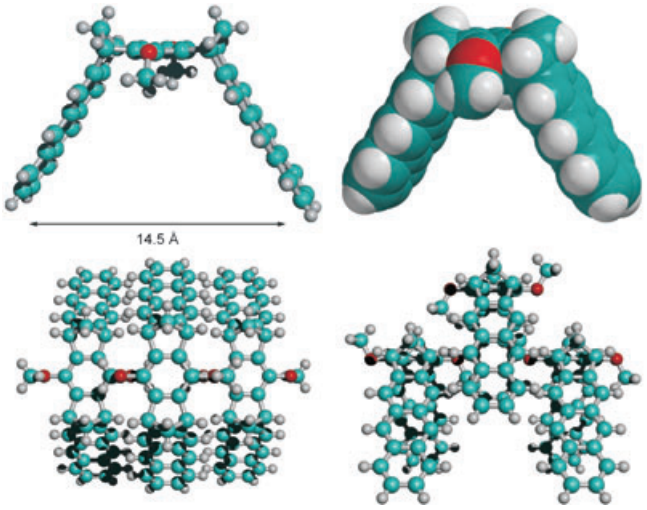

Figure 1. Single-crystal structure of the empty clip **1c**. Though the OMe groups are disordered, the analysis clearly shows that the OMe groups of one clip molecule point towards the cavities of the neighbor clip molecules, causing a widening of the clip cavity. The distance between the terminal carbon atoms is displayed in the structure (top, left).

NMR shift observed in the presence of the receptor and, hence, the weighted average of δ_0 and δ_C).[25] This report focuses on comparison of the complex stabilities and the structures of the anthracene clips **1a–c** with those of the naphthalene clips **2a–c**, the trimethylene-bridged clip **3**, and the tweezers **4a** and **4c** with respect to their dependence on the size and electrostatic properties of the substrate molecules **14–19**. Furthermore, the effect of the substituents at the central spacer unit of **1a–c** on the complex stability is determined and can be compared with the effect of substituents in the corresponding receptor systems **2a–c**.

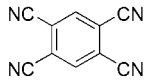

TCNB
14

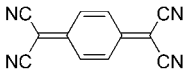

TCNQ
15

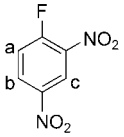

FDNB
16

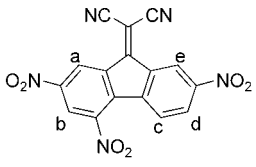

TNF
17

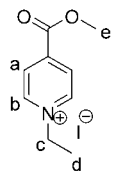

KS (Kosower Salt)
18

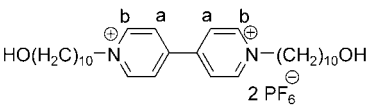

DeVio
19

The anthracene clips **1a–c** form complexes of different stability with the neutral and cationic substrate molecules **14–19**. In the case of compounds **16–19**, which possess nonequivalent protons, the association constants K_a and the maximum complexation-induced ^{1}H NMR shifts ($\Delta\delta_{max}$) were determined from the dependence of complexation-induced ^{1}H NMR shift ($\Delta\delta_{obs}$) of the substrate proton displaying the largest $\Delta\delta_{max}$ value. The $\Delta\delta_{max}$ values of the other substrate protons were then calculated from this value and the $\Delta\delta_{obs}$ values which were measured at the largest receptor concentration (see Experimental Section, Equation (5)). The results of ^{1}H NMR titration experiments are summarized in Table 1.

A Job-plot analysis was performed to determine the stoichiometry of the complex between the hydroquinone clip **1b** and TCNB (**14**) as a representative example (Figure 2).[26] The plot of the mole fraction χ ($\chi = [\mathbf{14}]_0/[\mathbf{1b}]_0+[\mathbf{14}]_0$) versus the mole fraction multiplied by the complexation-induced ^{1}H NMR shift of the observed substrate proton ($\chi \times \Delta\delta_{obs}$) shows a maximum at $\chi = 0.5$. This finding provides good evidence of a 1:1 complex stoichiometry. Additionally, evaluation of the ^{1}H NMR titration data observed for complex formation between hydroquinone clip **1b** as receptor and TCNB (**14**), TCNQ (**15**), TNF (**17**), and KS (**18**) as substrates by use of the HOSTEST program for various host–guest stoichiometries (1:1, 2:1, 1:2) gave reasonable fits only for the 1:1 stoichiometry.[25]

Comparison of the complex stabilities: The data summarized for the complex formation by the anthracene clips **1a–c** and by the naphthalene clips **2a–c** in Table 1 allow the following conclusions. All complexes of **1a–c** so far investigated are substantially more stable than the corresponding complexes of **2a–c**. A particularly strong effect on the complex stability is observed with substrates possessing extended arene units. For example, the TNF complex **17@1b** ($K_a = 4900\,\text{M}^{-1}$) is more stable than the corresponding complex **17@2b** ($K_a = 50\,\text{M}^{-1}$) by a factor of almost 100, whereas this factor between the TCNB complexes **14@1b** ($K_a = 12\,800\,\text{M}^{-1}$) and **14@2b** ($K_a = 2200\,\text{M}^{-1}$) is only of about 6. These results are good evidence that the larger van der Waals contact surfaces of the anthracene sidewalls in **1a–c** (in relation to the naphthalene side walls in **2a–c**) indeed lead to an increase in the complex stability. The electrostatic potential surfaces (EPSs) were calculated for the parent and hydroquinone anthracene and naphthalene clips **1** (R = H, OH) and **2** (R = H, OH) by quantum chemical methods (AM1, HF/6–31G**//AM1 and B3LYP/6–31G**//AM1) to be not very different from each other[27–31] (Figure 3). Evidently electrostatic effects are less important for the differences observed in the stabilities of the complexes with **1a–c** and **2a–c**.

The complexes of hydroquinone clip **1b** with **14–18** as substrates are more stable than those of the diacetoxy- or dimethoxy-substituted clips **1a** and **1c**, respectively.[32] The sequence of the complex stabilities (**1b** > **1a** > **1c**) resembles

Table 1. The maximum complexation-induced ^{1}H NMR shifts of the guest protons ($\Delta\delta_{max} = \delta_0 - \delta_{complex}$), association constants (K_a [M^{-1}]), and Gibbs enthalpies (ΔG [kcal mol^{-1}]) for the formation of host–guest complexes in $CDCl_3$ at 25 °C and 21 °C, respectively, for **2a–c**. The given errors are the results of standard deviation of the nonlinear regression with 95 % confidence.

Substrate	Receptor **1a**			Receptor **1b**			Receptor **1c**		
	K_a	ΔG	$\Delta\delta_{max}$	K_a	ΔG	$\Delta\delta_{max}$	K_a	ΔG	$\Delta\delta_{max}$
TCNB (**14**)	690 ± 30	−3.87	4.14	12 800 ± 700	−5.60	4.72	220 ± 10	−3.19	3.97
TCNQ (**15**)	130 ± 10	−2.88	2.36	640 ± 30	−3.83	3.35	40 ± 10	−2.18	1.28
FDNB (**16**)	20 ± 10	−1.77	3.32 (H_a) 2.44 (H_b) 2.26 (H_c)	30 ± 15	−2.01	2.85 (H_a) 2.88 (H_b) 2.51 (H_c)	10 ± 5	−1.36	2.65 (H_a) 2.17 (H_b) 2.00 (H_c)
TNF (**17**)	570 ± 30	−3.76	1.01 (H_a) 0.64 (H_b) 2.73 (H_c) 3.27 (H_d) 1.67 (H_e)	4900 ± 1000	−5.03	1.04 (H_a) 1.00 (H_b) 2.87 (H_c) 2.82 (H_d) 1.53 (H_e)	270 ± 20	−3.31	1.34 (H_a) 1.08 (H_b) 1.75 (H_c) 1.45 (H_d) 1.01 (H_e)
KS (**18**)	360 ± 40	−3.48	1.70 (H_a) 2.47 (H_b) 1.63 (H_c) 1.36 (H_d) 0.15 (H_e)	2300 ± 100	−4.58	3.25 (H_a) 3.09 (H_b) 0.97 (H_c) 0.56 (H_d) 0.02 (H_e)	90 ± 30	−2.66	0.96 (H_a) 1.27 (H_b) 0.46 (H_c) 0.43 (H_d) 0.14 (H_e)
DeVio **19**	120[a] ± 40	−2.83	2.11 (H_a) 1.53 (H_b)	70[a] ± 10	−2.51	2.34 (H_a) 1.29 (H_b)	< 10[a, b]	> −1.36	

Substrate	Receptor **2a**			Receptor **2b**			Receptor **2c**		
	K_a	ΔG	$\Delta\delta_{max}$	K_a	ΔG	$\Delta\delta_{max}$	K_a	ΔG	$\Delta\delta_{max}$
TCNB (**14**)	140 ± 10	−2.93	3.50	2200 ± 200	−4.56	3.57	< 10[c]	> −1.36	
TCNQ (**15**)	30 ± 10	−2.01	2.97	140 ± 10	−2.93	2.57	n. c. o.[d]		
FDNB (**16**)	30 ± 10	−2.01	1.83 (H_a) 1.38 (H_b) 0.74 (H_c)	–[e]			n. c. o.[d]		
TNF (**17**)	–[e]			50 ± 10	−2.32	0.50 (H_a) 0.65 (H_b) 2.23 (H_c) 2.81 (H_d) 1.23 (H_e)	–[e]		
KS (**18**)	140 ± 20	−2.93	1.82 (H_a) 2.40 (H_b)	1100 ± 110	−4.15	2.75 (H_a) 2.41 (H_b)	n. c. o.[d]		

[a] Solvent: $CDCl_3$/[D_6]acetone 1:1. [b] Estimated from the $\Delta\delta_{max}$ value of the complex **19@1b**. [c] Estimated from the $\Delta\delta_{max}$ value of the complex **14@2b**. [d] n.c.o. = no complexation observed. [e] Not yet examined.

that found for the corresponding naphthalene clips (**2b** > **2a** > **2c**). The effect of the substituents at the central benzene spacer unit of **2a–c** has been explained by their different steric sizes and conformations with respect to the clip cavity.[15] In the case of **2c**, the *syn*,*syn* conformation, in which both methoxy groups point toward the clip cavity, was calculated by force field to be the preferred one. In this conformation the sterically relatively large OMe substituents shield the clip cavity and hence disfavor complex formation. In the case of the diacetoxy-substituted system **2b** the *anti*, *anti* conformation was calculated to be the most stable one. In this conformation there is no steric hindrance to complex formation. In the single-crystal structures of some complexes of the diacetoxy-substituted clip **2a** or the tweezer **4a**, however, a *syn*,*anti* conformation is observed, in which the carbonyl oxygen atom (pointing toward the cavity) obviously enters into an additional attractive interaction with the guest molecule.[5] The finding that **2b** in most cases forms more stable complexes than **2a** and **2c** has been explained in terms of the smaller steric demand of the OH group (compared to the OAc and OMe groups) and its function as both donor and acceptor of hydrogen bonds to the guest molecule, leading to further complex stabilization additional to the arene–arene CH–π and π–π host–guest interactions. Evidently the same effects of the OAc, OH, and OMe groups on the complex stabilities are operative in the anthracene-walled clips **1a–c** and can also explain the differences in the complex stabilities observed for these systems.

Complex structures: The structure of the complex formed between TCNB (**14**) and the hydroquinone anthracene clip **1b** could be determined by single-crystal structure analysis

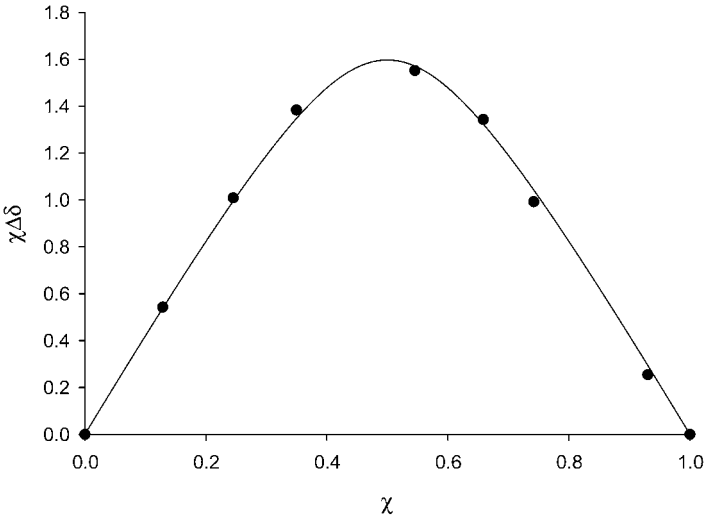

Figure 2. Job's plot for the complex **1b@14**.

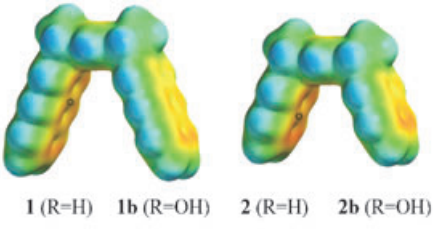

MEP [kcal mol^{-1}]

AM1	-23.1	-22.3	-23.6	-23.0
HF/6-31G**//AM1	-20.1	-19.4	-22.2	-20.7
B3LYP/6-31G**//AM1	-15.3	-14.7	-16.8	-16.1

Figure 3. Electrostatic potential surfaces (EPSs) of the parent anthracene clip **1** (R = H), left, and the parent naphthalene clip **2** (R = H), right, calculated by B3LYP/6–31G**//AM1. The color code ranges from −25 kcal mol^{-1} (red) to +25 kcal mol^{-1} (blue). The molecular electrostatic potentials (MEPs in kcal mol^{-1}) were calculated at the marked positions by AM1, HF/6–31G**//AM1, and B3LYP/6–31G**//AM1.[27]

(Figure 4). The interplanar angle between the mean planes of the anthracene moieties (max deviation 0.084 and 0.089 Å) is 4.8°, and the distance between the atoms C29 and the opposite C11 atom on the other side of the clip is 6.48 Å, while C30···C10 is 6.55 Å. The TCNB is positioned midway between the two anthracene units, and the closest intermolecular proximity of the outer walls of the anthracene units is 3.41 Å. Hydrogen bonds exist between the OH groups O1···O1′ (D = 2.88 Å, d = 2.05 Å, θ = 166°) linking the inversion-related molecules, whereas the oxygen atom O2 of the other OH group is linked to the cyano N1 of the TCNB (D = 3.05 Å, d = 2.34 Å, θ = 141°).

Comparison with the single-crystal structure of the empty clip **1c** demonstrates that the tips of the anthracene sidewalls are substantially compressed (by 8 Å) during the complex formation (from 14.5 Å to 6.5 Å) to provide attractive π–π interactions between TCNB (**14**) and the two anthracene units of **1b**. According to force field calculations, the expansion and compression of the aromatic sidewalls by bond angle distortion and out-of-plane deformation of the arene units in clips and tweezers of type **1**–**4** are low-energy processes;[27,33] in the anthracene clip **1b**, for example, expansion by 2 Å (from the calculated global minimum of 12.4 to 14.5 Å) and compression by 6 Å (from 12.5 to 6.5 Å) are calculated to require energies of 0.8 and 4.8 kcal mol^{-1}, respectively (Figure 5). The energy of compression is apparently overcompensated by the attractive noncovalent π–π host–guest interactions in the **14@1b** complex. The expansion observed in the single-crystal structure of **1c** seems to be an effect of the crystal lattice (Figure 1). Accordingly, the OMe groups of one clip molecule point toward the cavities of the neighbor molecule and cause its widening.

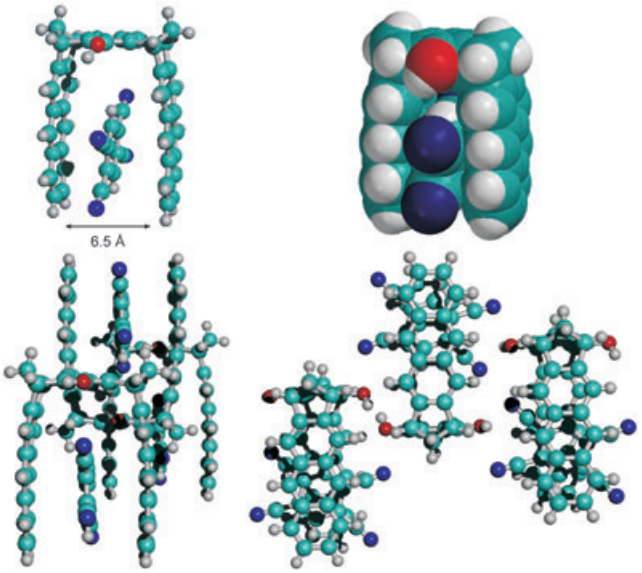

Figure 4. Single-crystal structure of the complex **14@1b** (CCDC-259882). The distance between the terminal carbon atoms in the structure is displayed (top, left).

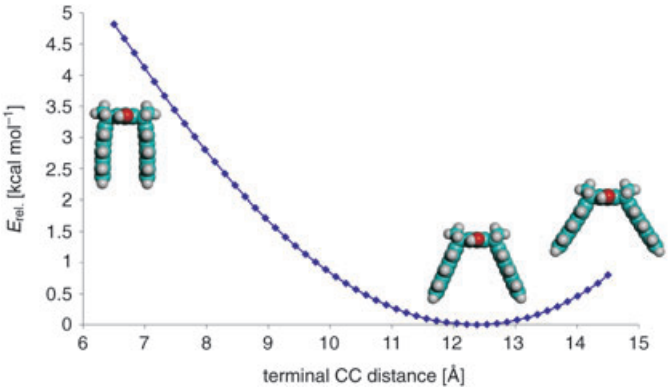

Figure 5. Energy profile for the compression of the anthracene sidewalls in clip **1b**, calculated by force field MMFF94.[27,33]

Beside the single-crystal structure analyses, the maximum complexation-induced ^{1}H NMR shifts ($\Delta\delta_{max}$) of guest pro-

tons in combination with quantum chemical shift calculations provide important information on the complex structures, as has been shown for the complex between *p*-dicyanobenzene and the parent naphthalene tweezer **4** (R = H).[7,34–36] In this study Monte-Carlo conformer searches using force fields were employed to calculate the complex structures. The force field calculations were calibrated with the known single-crystal structures of the complexes **14@1b** and **14@2b** (Figure 6, Table 2). Comparison of the calculated and the experimentally measured data (Table 2) indicates that the force fields MMFF94 and AMBER* (with and

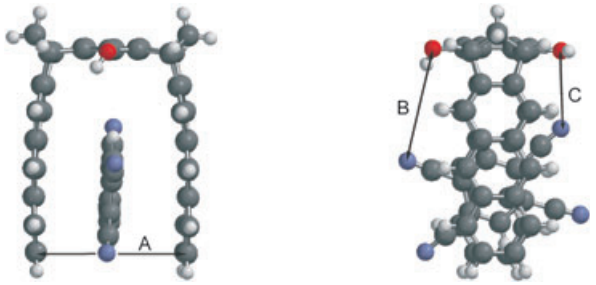

Figure 6. Nonbonding distances used to compare the force field structures with the single-crystal structure analysis.

Table 2. Comparison of the structures of the complexes **14@1b** and **14@2b** calculated with different force fields by Monte-Carlo conformer search (Macro Model 6.5, 5000 structures)[37,38] and those determined experimentally by single-crystal structure analysis. d = nonbonding distance between the atoms assigned in Figure 6, Δd = difference in the distance determined by calculation and that by single-crystal structure analysis ($\Delta d = d_{calcd} - d_{exptl}$).

	d (Δd) [Å]					
	Complex **14@1b**			Complex **14@2b**		
force field	A	B	C	A	B	C
MMFF94	8.17 (1.62)	3.07 (−1.87)	3.05 (−0.30)	8.44 (0.66)	3.01 (−0.11)	3.01 (−0.05)
MMFF94 ($CHCl_3$)	8.54 (1.99)	3.49 (−1.45)	2.92 (−0.43)	8.69 (0.91)	3.03 (−0.09)	3.01 (−0.05)
Amber*	6.68 (0.13)	3.22 (−1.72)	3.20 (−0.15)	7.20 (−0.58)	3.06 (−0.06)	3.06 (0.00)
Amber* ($CHCl_3$)	6.86 (0.31)	3.21 (−1.74)	3.19 (−0.16)	7.33 (−0.45)	3.07 (−0.06)	3.05 (−0.01)
crystal structure	6.55	4.94	3.35	7.78	3.13	3.06

without the addition of $CHCl_3$) both give reasonably good agreement with the experimental data. The distance A between the tips of complex **14@1b** (Figure 6) is better reproduced by AMBER* than by MMFF94, so we used AMBER* for further calculations. Larger deviations from the crystal data are observed for the N–O distances B and C between **14** and **1b** calculated by both force fields.

Inspection of the crystal lattice, however, shows that the TCNB molecule **14** is positioned unsymmetrically inside the cavity of **1b** in the crystal, because it forms intermolecular C≡N···H hydrogen bonds to the OH group of a neighbor clip molecule **1b** positioned upside down relative to the first one (Figure 4). In the complex **14@2b**,[5] in which only intramolecular C=N···H hydrogen bonds are observed, the calculated and experimentally determined distances B and C are in good accord.

Here we want to discuss only the structures of the more stable complexes for which the NMR titration experiments lead to reliable data for the $\Delta\delta_{max}$ values. In all three TNF complexes **17@1a–c** the protons (H_c and H_d) at the mononitro-substituted benzene ring show larger shifts than those (H_a and H_b) at the dinitro-substituted benzene ring, indicating that the complex structure in which the mononitro-substituted benzene ring is positioned inside the clip cavity (Figure 7 a), left) is the preferred one, contrary to the force field calculations for complex **17@1b** (which favor the positioning of the dinitro-substituted benzene ring inside the clip cavity) but in agreement with semiempirical PM3 calculations obtained by use of the optimized AMBER* geometries. Similar trends have been found in the calculations for the complexes formed between TNF (**17**) and the corresponding naphthalene clip **2b**, the trimethylene-bridged clip **3**, and the tetramethylene-bridged tweezer **4** (R = H). The calculated complex structures (Figure 7) nicely illustrate

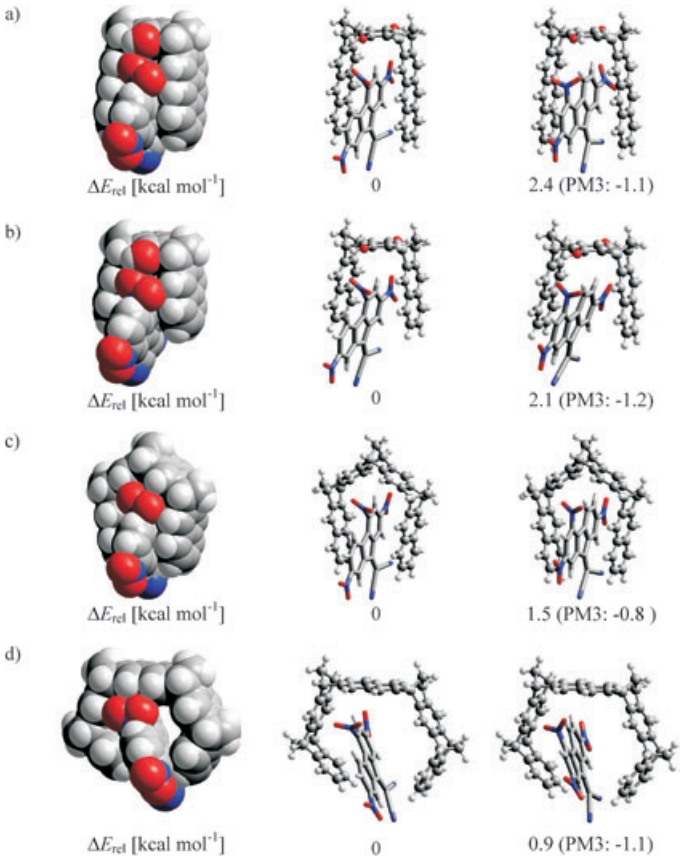

Figure 7. Structures and relative energies (ΔE_{rel}) of the conformers of: a) **17@1b**, b) **17@2b**, c) **17@3**, and d) **17@4** determined by a Monte-Carlo conformer search (MacroModel 6.5, Amber*, 5000 structures). The PM3 energies were determined in a single-point calculation by use of the Amber* geometries.

why only the anthracene clips **1a** and **1b** form stable complexes with TNF (**17**). The extended π surface of **17** is more fully embraced by the anthracene sidewalls of **1a** and **1b** than by the naphthalene side walls of clips **2** and **3**. In the structures calculated for complex **17@4** (R = H) (Figure 7d)) the guest molecule is clipped between the tweezer's tips, increasing the strain energy. In this case no complex formation could be detected by NMR.

The relatively subtle differences in the structures calculated for complexes of the Kosower salt **18** with clip **1a** and **1b** (Figure 8) can explain the different $\Delta\delta_{max}$ values observed

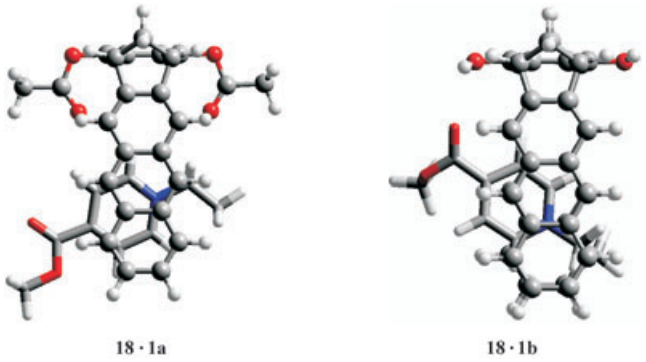

Figure 8. The lowest-energy structures of the complex structures **18@1a** (left) and **18@1b** (right) determined by a Monte-Carlo conformer search (MacroModel 6.5, 5000 structures).[37,38]

for the protons H_{a-d} in the complexes with **1a** and **1b** (Table 1). Evidently, because of an attractive interaction of the C=O function of one acetate group of clip **1a** with the positively charged nitrogen atom of the Kosower salt (KS) **18**, the $N^+-CH_2-CH_3$ group of **18** is calculated to point toward the central spacer unit of **1a** (Figure 8, left) leading to stronger shielding of the protons H_c and H_d by the magnetic anisotropy of the clip arene units than in the complex **18@1b**, in which a C=O···H–O hydrogen bond determines the position of the pyridinium ring of **18** inside the clip cavity away from the central spacer unit (Figure 8, right). In this case the protons H_c and H_d are less influenced by the clip arene units showing the smaller $\Delta\delta_{max}$ values. The C=O···H–O hydrogen bond is certainly one major reason why complex **18@1b** is substantially more stable than complex **18@1a**. In the case of the viologen **19** (also containing pyridinium rings) the complex **19@1b** does not have the structural feature to form a comparable hydrogen bond and is even less stable than complex **19@1a**.

Photophysical properties

Changes in the UV/Vis absorption spectra resulting from complex formation: The clips **1a–c** are colorless compounds showing absorption maxima in the range from 320 to 375 nm characteristic for anthracene moieties in their UV/VIS spectra (see Experimental Section).[39] A color change is observed when a guest molecule such as TCNB (**14**; colorless) or TNF (**17**; yellow) is added to a solution of **1a**, **1b**, or **1c**. The TCNB complexes of the diacetoxy- and dimethoxy-substituted clips **14@1a** and **14@1c** are red and that of the hydroquinone clip **14@1b** is purple, due to charge-transfer (CT) bands at λ_{max} = 503–528 nm. In the case of TNF complexes **17@1a**, **17@1b**, and **17@1c** the color again changes from yellow to green due to intense CT bands, this time at λ_{max} = 677–689 nm (Table 3). The complex of **1c** with the

Table 3. Absorption maxima and extinction coefficients of the charge-transfer complexes of the clips **1a–c** with TCNB (**14**) and TNF (**17**) and the clips **2a,b** with TCNB (**14**).

Complex	$c_{(Complex)}$ [mol L^{-1}]	λ_{max} CT	A	ε [l mol^{-1} cm]	log ε
14@1a	2.90×10^{-5}	503	0.053	1.84×10^{3}	3.26
14@1b	5.62×10^{-5}	528	0.071	1.26×10^{3}	3.10
14@1c	1.46×10^{-4}	515	0.126	8.65×10^{2}	2.93
17@1a	2.59×10^{-5}	677	0.021	8.16×10^{2}	2.91
17@1b	3.77×10^{-5}	689	0.016	4.13×10^{2}	2.62
17@1c	9.12×10^{-5}	685	0.082	9.06×10^{2}	2.96
14@2a	4.34×10^{-5}	416	0.061	1.40×10^{3}	3.15
14@2b	2.57×10^{-4}	416	0.424	1.65×10^{3}	3.22

solvatochromic Kosower salt **18** (frequently applied as a probe of solvent polarity)[40–45] does not show a significant change in color relative to pure **18** dissolved in $CHCl_3$. In the UV/Vis spectrum of a mixture of **1c** ($c_0 = 2.2\times10^{-4}$ M) and KS (**18**) ($c_0 = 2.4\times10^{-4}$ M) in $CHCl_3$ the bands assigned to **1c** and **18** are only superimposed. In the spectrum of a mixture of **1b** ($c_0 = 5.9\times10^{-5}$ M) and **18** ($c_0 = 5.9\times10^{-5}$ M), however, the shape and position of the band at the longest wavelength assigned to **18** are substantially changed. A shoulder at λ = 415 nm (log ε = 3.04) is observed for **18@1b** in $CHCl_3$ instead of the maximum at λ_{max} = 455 nm (log ε = 3.06) observed for pure **18** in $CHCl_3$. This blue shift of the CT band of **18** resulting from the complex formation with **1b** is similar to that observed in the complex of the naphthalene tweezer **4** (R = H) with **18** (from 455 nm of pure **18** to 425 nm in the complex **18@4**).[10]

On fluorescence measurements and spectrophotometric titration: The luminescence properties of clip **1b**, the guest TCNB (**14**), and the complex **14@1b** were also investigated. Figure 9 shows their absorption and emission spectra recorded in chloroform solution at room temperature. The receptor **1b** shows the structured fluorescence band typical of an anthracene-based species, with an emission lifetime of 1.0 ns. Under the same conditions, TCNB (**14**) features a less structured emission band, with a lifetime of 1.1 ns. In the solution containing both clip **1b** and TCNB (**14**) the intensity of luminescence emissions of these two separate components is much weaker, and a new, broader, weak, and structureless emission band due to the adduct **14@1b** is observed at 668 nm, with a lifetime of 4.2 ns. The luminescence properties of the complex **14@1b** can be interpreted as follows. The separate components **1b** and **14** fluoresce from their respective singlet excited states. In the adduct species **14@1b** a new charge-transfer state is present, and this

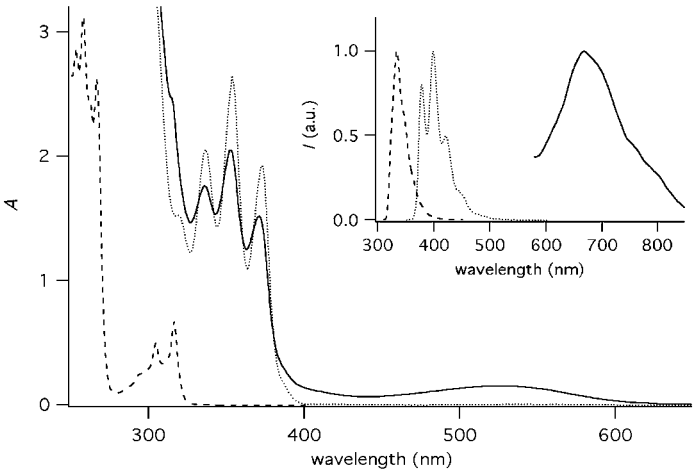

Figure 9. Room temperature absorption and luminescence (inset) spectra of 1.98×10^{-4} M chloroform solutions of the separate species **1b** (dotted line) and **14** (dashed line), and of a solution containing both **1b** and **14** (full line).

quenches the higher-energy singlets of the two components by energy transfer; as a result, only luminescence from this new CT state is observed. It is worth noting that the adduct **14@1b** represents, to the best of our knowledge, the first example of CT luminescence from a host–guest complex, although CT luminescence involving TCNB in donor–acceptor complexes and exciplexes is a known phenomenon.[46,47]

Changes in absorption and emission spectra can be exploited to obtain the association constant between the receptor **1b** and the guest TCNB (**14**). A titration experiment was performed by addition of **14** to a chloroform solution of **1b** and recording of the changes in the absorption and emission spectra of the solution. The most useful results were obtained from absorption measurements (see Supporting Information), as the luminescence of the complex **14@1b** is very weak and the signal is noisy. Figure 10 shows how the absorption intensity at 526 nm (due to formation of the complex **14@1b**) changes during the titration. These data were

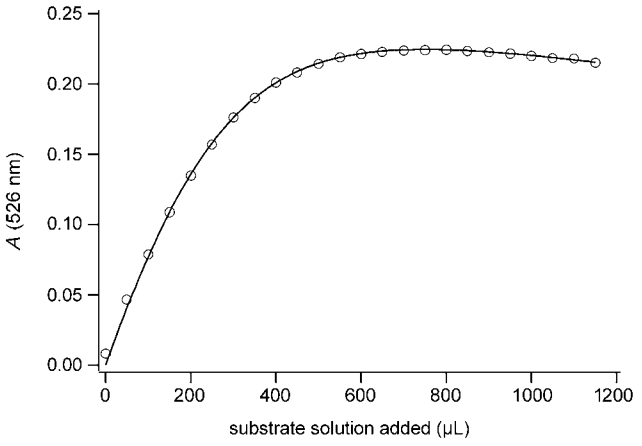

Figure 10. Absorbance due to the complex **14@1b** formed during titration of a solution of **1b** (3.01×10^{-4} M) with TCNB (**14**; 1.80×10^{-3} M, circles). The curve shows the fitting result, yielding $K_a = 1.24\times10^4$ M^{-1}.

fitted by standard methods, yielding a value of 1.24×10^4 L mol^{-1} for the association constant K_a. This value is in excellent agreement with that obtained independently from NMR measurements (Table 1). Analogous K_a values were also obtained by applying global analysis[48,49] to the full absorption spectra recorded during titration. The possibility of formation of other adducts was also taken into account, but worse fits was obtained on inclusion of adducts with 2:1 or 1:2 component ratio in the calculation. Thus, the one significant complex species is **14@1b**.

Conclusion

The novel molecular clips **1a–c** with anthracene sidewalls were synthesized by starting from bisdienophile **8a** and hexabromoxylene **9** and by a sequence of Diels–Alder reactions involving tetrabromo-*o*-quinodimethane as diene and a formal bisaryne as dienophile. They (particularly the hydroquinone clip **1b**) form stable host–guest complexes with a variety of electron-deficient guest molecules (**14–19**), even though the anthracene side walls have to be compressed substantially according to the single-crystal structure analyses of clip **1c** and of TCNB complex **14@1b** in order to provide attractive π–π interactions between the TCNB guest molecule and the two host anthracene sidewalls. The finding that the complexes of the clips **1a–c** are more stable than those of the corresponding clips **2a–c** can be explained by the larger van der Waals contact surfaces of the anthracene sidewalls in **1a–c** (in relation to the naphthalene sidewalls in **2a–c**). Color changes are observed in the complex formation between **1a–c** and TCNB (**14**)—from colorless to red or purple—and also with TNF—from yellow to green—resulting from charge-transfer (CT) bands of the corresponding complexes in the visible light range. The separate host **1b** and guest **14** fluoresce from their respective excited singlet states. In the complex **14@1b** the charge-transfer state quenches the higher-energy singlet states of the two components; as a result luminescence is only observed from this new CT state. To the best of our knowledge, adduct **14@1b** is the first example of CT luminescence from a host–guest complex.

Experimental Section

General remarks: IR: Bio-Rad FTS 135. UV/Vis: Varian Cary 300 Bio, Perkin–Elmer λ16. Luminescence spectra were recorded with a Perkin–Elmer LS-50 spectrofluorimeter, luminescence lifetimes were measured with an Edinburgh 199 single-photon counting apparatus. ^{1}H NMR, ^{13}C NMR, DEPT H, H-COSY, C, H-COSY, NOESY, HMQC, HMBC: Bruker DRX 500. ^{1}H NMR titration experiments: Varian Gemini XL 200 and Bruker DRX 500; the undeuterated portion of the solvent was used as an internal reference. Positions of the protons of the methano bridges are indicated by the letters *i* (*innen*, towards the center of the molecule) and *a* (*aussen*, away from the center of the molecule). MS: Fison Instruments VG ProSpec 3000 (70 eV). All melting points are uncorrected. Column chromatography: silica gel 0.063–0.2 mm. All solvents were distilled prior to use.

7,16-Diacetoxy-2,3,11,12-tetrabromo-(6a,8a,15a,17a)-6,8,15,17-tetrahydro-6,17:8,15-dimethanoheptacene (12a): A mixture of bisdienophile **8a** (4 g, 12.41 mmol), α,α,α′,α′,4,5-hexabromo-*o*-xylene (**9**, 56 g, 96.62 mmol), anhydrous NaI (92 g, 613.78 mmol), anhydrous $CaCO_3$ (20 g, 199.82 mmol), and anhydrous dimethyl formamide (300 mL) was stirred under argon for 30 min at room temperature and then heated to 55 °C under vacuum (100 mbar) for 5 h. The reaction mixture was poured into ice (1200 g) and the brown mixture, after decolorization by addition of aqueous sodium hydrogen sulfite, was extracted with dichloromethane (3×200 mL), and the combined organic layers were filtered, washed with saturated aqueous sodium hydrogen carbonate (200 mL) and water (5×400 mL), dried over $MgSO_4$, and concentrated in vacuo in a rotary evaporator. Purification by column chromatography on silica gel with a mixture of EtOAc/cyclohexane (1:3) as eluent gave **12a** (6.76 g, 8.07 mmol, 65 %) as a light brown solid. m.p. > 300 °C; ^{1}H NMR (500 MHz, $CDCl_3$): δ = 2.41 (d, ^2J(19a-H, 19i-H) = 8 Hz, 2H; 19a-H, 20a-H), 2.47 (s, 6H; $-CH_3$), 2.63 (d, 2H; 19i-H, 20i-H), 4.27 (s, 4H; 6-H, 8-H, 15-H, 17-H), 7.51 (s, 4H; 1-H, 4-H, 10-H, 13-H), 7.75 ppm (s, 4H; 5-H, 9-H, 14-H, 18-H); ^{13}C NMR (125 MHz, $CDCl_3$): δ = 20.84 (q; $-CH_3$), 48.01 (d; C-6, C-8, C-15, C-17), 64.59 (t; C-19, C-20), 119.03 (d; C-5, C-9, C-14, C-18), 121.02 (s; C-2, C-3, C-11, C-12), 131.75 (d; C-1, C-4, C-10, C-13), 131.86 (s; C-4a, C-9a, C-13a, C-18a), 137.28 (s; C-7, C-16), 140.43 (s; C-6a, C-7a, C-15a, C-16a), 147.21 (s; C-5a, C-8a, C-14a, C-17a), 168.44 ppm (s; C=O); IR (KBr): $\tilde{\nu}$ = 3014 (CH), 2991 (CH), 2939 (CH), 1765 (C=O), 1205 cm^{-1} (C−O); UV/Vis ($CHCl_3$): λ_{max} (lgε) = 275 (4.37), 286 (4.28), 319 (3.53), 334 nm (3.57); MS (70 eV): *m*/*z* (%): 838 (74) $[M]^+$, 796 (34) $[M-CH_2CO]^+$, 754 (100) $[M-2CH_2CO]^+$, 43 (90) $[CH_3CO]^+$, isotopic pattern = 834 (17), 836 (66), 838 (100), 840 (69), 842 (20); HR-MS (70 eV): found 833.825; $C_{36}H_{22}O_4Br_4$ calcd 833.822.

2,3,11,12-Tetrabromo-7,16-dimethoxy-(6a,8a,15a,17a)-6,8,15,17-tetrahydro-6,17:8,15-dimethanoheptacene (12c): A suspension of **12a** (6 g, 7.16 mmol), phenylhydrazine (800 mg, 7.39 mmol), and powdered KOH (3 g, 53.47 mmol) in isopropanol (250 mL) was stirred under argon for 3 h at room temperature. After addition of potassium *tert*-butoxide (1.2 g, 10.69 mmol) and methyl iodide (6 mL, 96.37 mmol), the reaction mixture was stirred for an additional 3 h at room temperature. HCl (500 mL, 1 M) was added slowly, and the precipitate was filtered and dried over P_2O_5. Purification by column chromatography on silica gel with a mixture of chloroform/*n*-hexane (1:1) as eluent gave **12c** (5.04 g, 6.44 mmol, 90 %) as a light yellow solid. m.p. > 300 °C; ^{1}H NMR (500 MHz, $CDCl_3$): δ = 2.40 (d, ^2J(19a-H, 19i-H) = 8 Hz, 2H; 19a-H, 20a-H), 2.53 (d, 2H; 19i-H, 20i-H), 3.80 (s, 6H; $-OCH_3$), 4.52 (s, 4H; 6-H, 8-H, 15-H, 17-H), 7.36 (s, 4H; 5-H, 9-H, 14-H, 18-H), 7.76 ppm (s, 4H; 1-H, 4-H, 10-H, 13-H); ^{13}C NMR (125 MHz, $CDCl_3$): δ = 47.55 (d; C-6, C-8, C-15, C-17), 61.31 (q; $-OCH_3$), 63.87 (t; C-19, C-20), 118.28 (d; C-5, C-9, C-14, C-18), 121.01 (d; C-2, C-3, C-11, C-12), 131.67 (d; C-1, C-4, C-10, C-13), 131.89 (s; C-4a, C-9a, C-13a, C-18a), 139.30 (s; C-6a, C-7a, C-15a, C-16a), 145.51 (s; C-5a, C-8a, C-14a, C-17a), 148.76 ppm (s; C-7, C-16); IR (KBr): $\tilde{\nu}$ = 3020 (CH), 2994 (CH), 2935 (CH), 2884 (CH), 1581 (C=C), 1289 cm^{-1} (C−O); UV/Vis ($CHCl_3$): λ_{max} (lgε) = 265 (4.63), 320 (3.59), 335 nm (3.67); MS (70 eV): *m*/*z* (%): 782 (100) $[M]^+$, 767 (26) $[M-CH_3]^+$, 702 (11) $[M-Br]^+$, 622 (12) $[M-2\times Br]^+$, isotopic pattern = 778 (16), 780 (64), 782 (100), 784 (72), 786 (19); HR-MS (70 eV): found 777.835; $C_{34}H_{22}O_2Br_4$ calcd 777.838.

Direct synthesis of 2,3,11,12-tetrabromo-7,16-dimethoxy-(6a,8a,15a,17a)-6,8,15,17-tetrahydro-6,17:8,15-dimethanoheptacene (12c): The mixture of bisdienophile **8c** (3 g, 11.27 mmol), α,α,α′,α′,4,5-hexabromo-*o*-xylene (**9**, 40 g, 69.01 mmol), anhydrous NaI (55 g, 366.93 mmol), and anhydrous dimethyl formamide (220 mL) was stirred at 65 °C under vacuum (100 mbar) for 19 h. The reaction mixture was poured into ice (500 g) and the brown mixture, after decolorization by addition of aqueous sodium hydrogen sulfite, was extracted with dichloromethane (3×200 mL), and the combined organic layers were filtered, washed with saturated aqueous sodium hydrogen carbonate (250 mL) and water (5×400 mL), dried over $MgSO_4$, and concentrated in vacuo in a rotary evaporator. Purification by column chromatography on silica gel with a mixture of EtOAc/cyclohexane (1:3) as eluent gave crude **12c** (3.4 g). [Because of the low polarity of **12c** the separation was unsatisfactory and required a long column (40×1000 mm)]. Recrystallization of the crude product from an ethanol/dichloromethane mixture gave **12c** (2.91 g, 3.73 mmol, 34 %) as a light yellow solid. The spectroscopic data of **12c** prepared by the direct synthesis are equivalent to those of **12c** prepared by the two-step synthesis.

8,19-Dimethoxy-(1α,4α,7α,9α,12α,15α,18α,20α)-1,4,7,9,12,15,18,20-octahydro-1,4:12,15-dioxa-7,20:9,18-dimethanononacene (*syn*/*syn*-13c), 8,19-dimethoxy-(1β,4β,7α,9α,12α,15α,18α,20α)-1,4,7,9,12,15,18,20-octahydro-1,4:12,15-dioxa-7,20:9,18-dimethanononacene (*syn*,*anti*-13c), and 8,19-dimethoxy-(1β,4β,7α,9α,12β,15β,18α,20α)-1,4,7,9,12,15,18,20-octahydro-1,4:12,15-dioxa-7,20:9,18-dimethanononacene (*anti*,*anti*-13c): *n*BuLi (13.76 mmol in 175 mL *n*-hexane) was added dropwise at −78 °C under argon over 5 h to a stirred solution of **12c** (5 g, 6.39 mmol) and furan (freshly distilled over CaH_2, 40 mL, 552.29 mmol) in dry THF (500 mL). The mixture was allowed to warm up slowly (overnight) to room temperature, and methanol (2 mL) was added. After removal of the solvents in vacuo in a rotary evaporator, the residue was purified by column chromatography on silica gel with EtOAc/cyclohexane (1:3) as eluent to give the isomers of **13c** (isomer ratio 1:4:2) (1.53 g, 2.56 mmol, 40 %) as a colorless solid. M.p. decomp > 250 °C; NMR data see below; IR (KBr): $\tilde{\nu}$ = 3082 (C−H), 3003 (C−H), 2962 (C−H), 2930 (C−H), 2850 (C−H), 2826 (C−H), 1478 (C=C), 1277 cm^{-1} (C−O); UV/Vis ($CHCl_3$): λ_{max} (lgε) = 243 (4.71), 317 (3.32), 331 nm (3.37); MS (70 eV): *m*/*z* (%): 598 (100) $[M]^+$, 583 (40) $[M-CH_3]^+$, 567 (21) $[M-OCH_3]$; HR-MS (70 eV): found 598.215; $C_{42}H_{30}O_4$ calcd 598.214.

Analytical samples of the pure isomers can be obtained by liquid chromatography by use of a thin but long column (10×300 mm) and with EtOAc/cyclohexane (1:3) as eluent.

syn,*anti*-**13c**: ^{1}H NMR (500 MHz, $CDCl_3$): δ = 2.38, 2.45 (dt, ^2J(23a-H, 23i-H) = 6.6 Hz, ^3J(23a-H, 9-H) = 1.5 Hz, 2H; 23a-H, 24a-H), 2.49, 2.51 (dt, ^3J(23i-H, 9-H) = 1.5 Hz, 2H; 23i-H, 24i-H), 3.77 (s, 6H; $-OCH_3$), 4.47, 4.49 (t, 4H; 7-H, 9-H, 18-H, 20-H), 5.62, 5.65 (s, 4H; 1-H, 4-H, 12-H, 15-H), 6.72, 6.88 (s, 4H; 2-H, 3-H, 13-H, 14-H), 7.32, 7.33 (s, 4H; 5-H, 11-H, 16-H, 22-H), 7.38, 7.40 ppm (s, 4H; 6-H, 10-H, 17-H, 21-H); ^{13}C NMR (125 MHz, $CDCl_3$): δ = 47.58 (d; C-7, C-9, C-18, C-20), 61.21 (q; $-OCH_3$), 64.15, 64.46 (t; C-23, C-24), 81.80, 81.82 (d; C-1, C-4, C-12, C-15), 118.55, 118.71 (d; C-5, C-11, C-16, C-22), 120.06, 120.11 (d; C-6, C-10, C-17, C-21), 130.11, 130.15 (s; C-5a, C-10a, C-16a, C-21a), 139.87, 140.03 (s; C-7a, C-8a, C-18a, C-19a), 141.80, 141.86 (d; C-2, C-3, C-13, C-14), 143.99, 144.09 (s; C-4a, C-11a, C-15a, C-22a), 145.38 (s; C-8, C-19), 147.98, 148.01 ppm (s; C-6a, C-9a, C-17a, C-20a).

syn,*syn*-**13c** or *anti*,*anti*-**13c**: ^{1}H NMR (500 MHz, $CDCl_3$): δ = 2.43 (dt, ^2J(23a-H, 23i-H) = 8 Hz, ^3J(23a-H, 9-H) = 1.5 Hz, 2H; 23a-H, 24a-H), 2.50 (dt, ^3J(23i-H, 9-H) = 1.5 Hz, 2H; 23i-H, 24i-H), 3.74 (s, 6H; $-OCH_3$), 4.47 (t; 4H; 7-H, 9-H, 18-H, 20-H), 5.65 (s, 4H; 1-H, 4-H, 12-H, 15-H), 6.74 (s, 4H; 2-H, 3-H, 13-H, 14-H), 7.31 (s, 4H; 5-H, 11-H, 16-H, 22-H), 7.37 ppm (s, 4H; 6-H, 10-H, 17-H, 21-H); ^{13}C NMR (125 MHz, $CDCl_3$): δ = 47.53 (d; C-7, C-9, C-18, C-20), 61.14 (q; $-OCH_3$), 64.03 (t; C-23, C-24), 81.80 (d; C-1, C-4, C-12, C-15), 118.66 (d; C-5, C-11, C-16, C-22), 120.06 (d; C-6, C-10, C-17, C-21), 130.11 (s; C-5a, C-10a, C-16a, C-21a), 140.04 (s; C-7a, C-8a, C-18a, C-19a), 141.83 (d; C-2, C-3, C-13, C-14), 143.88 (s; C-4a, C-11a, C-15a, C-22a), 145.33 (s; C-8, C-19), 148.04 ppm (s; C-6a, C-9a, C-17a, C-20a).

syn,*syn*-**13c** or *anti*,*anti*-**13c**: ^{1}H NMR (500 MHz, $CDCl_3$): δ = 2.37 (d, ^2J(23a-H, 23i-H) = 8 Hz, 2H; 23a-H, 24a-H), 2.49 (d, 2H; 23i-H, 24i-H), 3.80 (s, 6H; $-OCH_3$), 4.49 (s, 4H; 7-H, 9-H, 18-H, 20-H), 5.64 (s, 4H; 1-H, 4-H, 12-H, 15-H), 6.88 (s, 4H; 2-H, 3-H, 13-H, 14-H), 7.34 (s, 4H; 5-H, 11-H, 16-H, 22-H), 7.42 ppm (s, 4H; 6-H, 10-H, 17-H, 21-H); ^{13}C NMR (125 MHz, $CDCl_3$): δ = 47.66 (d; C-7, C-9, C-18, C-20), 61.36 (q; $-OCH_3$), 65.03 (t; C-23, C-24), 81.80 (d; C-1, C-4, C-12, C-15), 118.60 (d; C-5, C-11, C-16, C-22), 120.02 (d; C-6, C-10, C-17, C-21), 130.16 (s; C-5a, C-10a, C-16a, C-21a), 139.74 (s; C-7a, C-8a, C-18a, C-19a), 141.90 (d; C-2, C-3, C-13, C-14), 144.18 (s; C-4a, C-11a, C-15a, C-22a), 145.43 (s; C-8, C-19), 147.88 ppm (s; C-6a, C-9a, C-17a, C-20a).

8,19-Dimethoxy-(7α,9α,18α,20α)-7,9,18,20-tetrahydro-7,20:9,18-dimethanononacene (1c): Zinc powder (650 mg, 9.94 mmol) was added under argon to a stirred suspension of $TiCl_4$ (1.5 g, 4.49 mmol, $TiCl_4$·2THF complex) in dry THF (35 mL). The gray suspension was heated to reflux and a suspension of the isomeric mixture of **13c** (500 mg, 0.84 mmol) in dry

THF (20 mL) was added dropwise. After the mixture had been heated at reflux for 8 h, the cooled mixture was poured into HCl (100 mL, 1 M). The purple mixture was extracted with dichloromethane (5×70 mL), and the extract was washed with water (2×50 mL) and dried over $MgSO_4$. Solvent removal gave a solid, which was filtered on silica gel with EtOAc/cyclohexane (1:3) as eluent. Recrystallization of the crude product from an ethanol/chloroform mixture gave **1c** (305 mg, 0.54 mmol, 64%) as colorless crystals. m.p. > 300 °C; ^{1}H NMR (500 MHz, $CDCl_3$): δ = 2.42 (dt, ^2J(23a-H, 23i-H) = 8 Hz, ^3J(23a-H, 9-H) = 1.4 Hz, 2H; 23a-H, 24a-H), 2.54 (dt, ^3J(23i-H, 9-H) = 1.4 Hz, 2H; 23i-H, 24i-H), 3.87 (s, 6H; $-OCH_3$), 4.57 (t; 4H; 7-H, 9-H, 18-H, 20-H), 7.28 (m, 4H; 2-H, 3-H, 13-H, 14-H), 7.62 (s, 4H; 6-H, 10-H, 17-H, 21-H), 7.78 (m, 4H; 1-H, 4-H, 12-H, 15-H), 8.07 ppm (s, 4H; 5-H, 11-H, 16-H, 22-H); ^{13}C NMR (125 MHz, $CDCl_3$): δ = 47.36 (d; C-7, C-9, C-18, C-20), 61.29 (q; $-OCH_3$), 62.42 (t; C-23, C-24), 118.91 (d; C-6, C-10, C-17, C-21), 124.75 (d; C-2, C-3, C-13, C-14), 125.62 (d; C-5, C-11, C-16, C-22), 127.72 (d; C-1, C-4, C-12, C-15), 130.88 (s; C-5a, C-10a, C-16a, C-21a), 131.41 (s; C-4a, C-11a, C-15a, C-22a), 139.27 (s; C-7a, C-8a, C-18a, C-19a), 145.35 (s; C-8, C-19), 146.24 ppm (s; C-6a, C-9a, C-17a, C-20a); IR (KBr): $\tilde{\nu}$ = 3046 (CH), 3014 (CH), 2954 (CH), 2927 (CH), 2855 (CH), 2828 (CH), 1486 (C=C), 1293 cm^{-1} (C–O); UV/Vis ($CHCl_3$): λ_{max} (lg ε) = 321 (3.87), 337 (4.05), 354 (4.11), 373 nm (3.98); MS (70 eV): *m/z* (%): 566 (100) $[M]^+$, 551 (31) $[M-CH_3]^+$, 535 (8) $[M-OCH_3]^+$; HR-MS (70 eV): found 566.228; $C_{42}H_{30}O_2$ calcd 566.225.

8,19-Dihydroxy-(7α,9α,18α,20α)-7,9,18,20-tetrahydro-7,20:9,18-dimethanononacene (1b): Under argon, a stirred solution of **1c** (100 mg, 0.18 mmol) in dichloromethane (17 mL) was cooled down to −78 °C and treated with boron tribromide (500 μL, 5.19 mmol). The solution was allowed to warm up slowly to room temperature over 24 h. Methanol (1 mL) was slowly added to the solution, which was cooled again with ice/water to quench the excess of boron tribromide. After removal of the solvents, **1b** (95 mg, 0.18 mmol, 98%) was isolated as a light gray solid. For further purification, **1b** was reprecipitated from chloroform by addition of *n*-hexane. m.p. > 300 °C; ^{1}H NMR (500 MHz, $CDCl_3$): δ = 2.43 (dt, ^2J(23a-H, 23i-H) = 8 Hz, ^3J(23a-H, 9-H) = 1.3 Hz, 2H; 23a-H, 24a-H), 2.55 (dt, ^3J(23i-H, 9-H) = 1.3 Hz, 2H; 23i-H, 24i-H), 4.39 (s, 2H; −OH), 4.48 (t; 4H; 7-H, 9-H, 18-H, 20-H), 7.26 (m, 4H; 2-H, 3-H, 13-H, 14-H), 7.55 (s, 4H; 6-H, 10-H, 17-H, 21-H), 7.75 (m, 4H; 1-H, 4-H, 12-H, 15-H), 7.97 ppm (s, 4H; 5-H, 11-H, 16-H, 22-H); ^{13}C NMR (125 MHz, $CDCl_3$): δ = 46.55 (d; C-7, C-9, C-18, C-20), 62.94 (t; C-23, C-24), 119.05 (d; C-6, C-10, C-17, C-21), 124.67 (d; C-2, C-3, C-13, C-14), 125.58 (d; C-5, C-11, C-16, C-22), 127.73 (d; C-1, C-4, C-12, C-15), 130.75 (s; C-5a, C-10a, C-16a, C-21a), 131.34 (s; C-4a, C-11a, C-15a, C-22a), 134.02 (s; C-7a, C-8a, C-18a, C-19a), 138.87 (s; C-8, C-19), 145.34 ppm (s; C-6a, C-9a, C-17a, C-20a); IR (KBr): $\tilde{\nu}$ = 3417 (OH), 3048 (CH), 2990 (CH), 2967 (CH), 2934 (CH), 2859 (CH), 1486 (C=C), 1293 cm^{-1} (C–O); UV/Vis ($CHCl_3$): λ_{max} (lg ε) = 319 (3.74), 336 (3.89), 353 (4.01), 372 nm (3.86); MS (70 eV): *m/z* (%): 538 (100) $[M]^+$; HR-MS (70 eV): found 538.191; $C_{40}H_{26}O_2$ calcd 538.193.

8,19-Diacetoxy-(7α,9α,18α,20α)-7,9,18,20-tetrahydro-7,20:9,18-dimethanononacene (1a): Freshly distilled acetic anhydride (6 mL, 63.45 mmol) was added under argon to a stirred solution of **1b** (300 mg, 0.56 mmol) in pyridine (75 mL). The solution was stirred for 24 h at room temperature and then poured into ice/water (300 mL). The precipitate was filtered and dried over P_2O_5. Purification by column chromatography on silica gel with a mixture of EtOAc/cyclohexane (1:3) as eluent gave **1a** (216 mg, 0.35 mmol, 63%) as a colorless solid. m.p. > 300 °C; ^{1}H NMR (500 MHz, $CDCl_3$): δ = 2.42 (dt, ^2J(23a-H, 23i-H) = 8.3 Hz, ^3J(23a-H, 9-H) = 1.4 Hz, 2H; 23a-H, 24a-H), 2.52 (s, 6H; $-CH_3$), 2.67 (dt, ^3J(23i-H, 9-H) = 1.5 Hz, 2H; 23i-H, 24i-H), 4.32 (s, 4H; 7-H, 9-H, 18-H, 20-H), 7.28 (m, 4H; 2-H, 3-H, 13-H, 14-H), 7.62 (s, 4H; 6-H, 10-H, 17-H, 21-H), 7.79 (m, 4H; 1-H, 4-H, 12-H, 15-H), 8.08 ppm (s, 4H; 5-H, 11-H, 16-H, 22-H); ^{13}C NMR (125 MHz, $CDCl_3$): δ = 20.91 (q; $-CH_3$), 47.89 (d; C-7, C-9, C-18, C-20), 63.19 (t; C-23, C-24), 119.65 (d; C-6, C-10, C-17, C-21), 124.74 (d; C-2, C-3, C-13, C-14), 125.76 (d; C-5, C-11, C-16, C-22), 127.78 (d; C-1, C-4, C-12, C-15), 130.86 (s; C-5a, C-10a, C-16a, C-21a), 131.42 (s; C-4a, C-11a, C-15a, C-22a), 137.18 (s; C-7a, C-8a, C-18a, C-19a), 140.29 (s; C-8, C-19), 144.68 (s; C-6a, C-9a, C-17a, C-20a), 168.64 ppm (s; C=O); IR (KBr): $\tilde{\nu}$ = 3050 (CH), 3015 (CH), 2992 (CH), 2967 (CH), 2934 (CH), 2859 (CH), 1773 (C=O), 1211 cm^{-1} (C–O); UV/Vis ($CHCl_3$): λ_{max} (lg ε) = 321 (3.76), 336 (3.98), 353 (4.09), 373 nm (3.95); MS (70 eV): *m/z* (%): 622 (100) $[M]^+$, 580 (30) $[M-CH_2CO]^+$, 538 (70) $[M-2CH_2CO]$; HR-MS (70 eV); found 622.210; $C_{44}H_{30}O_4$ calcd 622.214.

Determination of K_a—^{1}H NMR titration method: Receptor R and substrate S are in equilibrium with the 1:1 complex RS (R + S ⇄RS). The association constant K_a is then defined by Equation (1). $[R]_0$ and $[S]_0$ are the starting concentrations of the receptor and the substrate, respectively.

$$K_a = \frac{[RS]}{[R]\times[S]} = \frac{[RS]}{([R]_0-[RS])\times([S]_0-[RS])} \quad (1)$$

The observed chemical shift (δ_{obs}) of the substrate in the ^{1}H NMR spectrum is an averaged value between free (δ_0) and complexed substrate (δ_{RS}), provided that the exchange is fast on the NMR time scale ([Eq. (2)]). Combination of Equations (1) and (2) and the use of differences in chemical shift ($\Delta\delta = \delta_0-\delta_{obs}$; $\Delta\delta_{max} = \delta_0-\delta_{RS}$) leads to Equation (3).

$$\delta_{obs} = \frac{[S]}{[S]+[RS]}\times\delta_0 + \frac{[RS]}{[S]+[RS]}\times\delta_{RS} \quad (2)$$

$$\Delta\delta = \frac{\Delta\delta_{max}}{[S]_0}\times\left(\frac{1}{2}\left([R]_0+[S]_0+\frac{1}{K_a}\right) - \sqrt{\frac{1}{4}\times\left([R]_0+[S]_0+\frac{1}{K_a}\right)^2-[R]_0\times[S]_0}\right) \quad (3)$$

In the titration experiments, the total substrate concentration $[S]_0$ was kept constant, whereas the total receptor concentration $[R]_0$ was varied. This was achieved by dissolving a defined amount of the receptor R in 0.6 mL of a solution containing the substrate concentration $[S]_0$. $\Delta\delta$ was determined from the chemical shift of the pure substrate and the chemical shift of the substrate measured in the ^{1}H NMR spectrum (500 MHz, 25 °C for R = **1a–c** and 200 MHz, 24 °C for R = **2a–c**) of this mixture. Successive addition of further solution containing $[S]_0$ leads to a dilution of the concentration $[R]_0$ in the mixture while $[S]_0$ is kept constant. Measurement of the chemical shift of the substrate-dependence on the concentration $[R]_0$ afforded the data pairs $\Delta\delta$ and $[R]_0$. Fitting of these data to the (1:1) binding isotherm by iterative methods[25] delivered the parameters K_a and $\Delta\delta_{max}$

In the case of substrates possessing two or more nonequivalent protons, the determination of the association constants K_a sometimes leads to different values of K_a. This may result from increasing errors caused by decreasing $\Delta\delta_{max}$ values. To minimize such errors the association constants K_a were determined for that proton of the substrate S displaying the largest value of $\Delta\delta_{max}$ [Eq. (4)]. The $\Delta\delta_{max}$ values of the other substrate protons were calculated by the use of Equation (5).

$$[RS] = [S]_0\frac{\Delta\delta_1}{\Delta\delta_{1,max}} = [S]_0\frac{\Delta\delta_2}{\Delta\delta_{2,max}} = [S]_0\frac{\Delta\delta_n}{\Delta\delta_{n,max}} \quad (4)$$

$$\Rightarrow \Delta\delta_{n,max} = \Delta\delta_n\frac{\Delta\delta_1}{\Delta\delta_{1,max}} \quad (5)$$

From the corresponding relationship between the concentrations of the receptor $[R]_0$ and the complex [RS] the maximum complexation-induced shifts ($\Delta\delta_{R,max}$) for the protons of the receptor R can be calculated by use of Equation (6).

$$[RS] = [S]_0\frac{\Delta\delta_1^S}{\Delta\delta_{1,max}^S} = [R]_0\frac{\Delta\delta_1^R}{\Delta\delta_{1,max}^R} \Rightarrow \Delta\delta_{1,max}^R = \frac{[R]_0}{[S]_0}\Delta\delta_1^R\frac{\Delta\delta_{1,max}^S}{\Delta\delta_1^S} \quad (6)$$

The results of ^{1}H NMR titration experiments are given in the Supporting Information.

Crystal structure determinations: CCDC-259881 and CCDC-259882 contain the supplementary crystallographic data for this paper. These data

can be obtained free of charge from the Cambridge Crystallographic Data Centre via www.ccdc.cam.ac.uk/data_request/cif.

Acknowledgements

This work was supported by the Deutsche Forschungsgemeinschaft (Sonderforschungsbereich SFB 452). We thank Willi Sicking for the assistance with the HOSTEST calculations, and Professor Craig Wilcox for providing us access to the HOSTEST program.

[1] J. M. Lehn, *Supramolecular Chemistry. Concepts and Perspectives*, VCH, Weinheim, **1995**.
[2] H.-J. Schneider, A. Yatsimirsky, *Principles and Methods in Supramolecular Chemistry*, Wiley-VCH, Weinheim, **2000**.
[3] J. L. Atwood, J. W. Steed, *Supramolecular Chemistry*, Wiley, Weinheim, **2000**.
[4] E. A. Meyer, R. K. Castellano, F. Diederich, *Angew. Chem.* **2003**, *115*, 1244–1287; *Angew. Chem. Int. Ed.* **2003**, *42*, 1210–1250.
[5] F.-G. Klärner, J. Panitzky, D. Bläser, R. Boese, *Tetrahedron* **2001**, *57*, 3673–3687.
[6] F.-G. Klärner, M. Lobert, U. Naatz, H. Bandmann, R. Boese, *Chem. Eur. J.* **2003**, *9*, 5036–5047.
[7] F.-G. Klärner, U. Burkert, M. Kamieth, R. Boese, J. Benet-Buchholz, *Chem. Eur. J.* **1999**, *5*, 1700–1707.
[8] M. Kamieth, F.-G. Klärner, *J. Prakt. Chem.* **1999**, *341*, 245–251.
[9] M. Kamieth, U. Burkert, P. S. Corbin, S. J. Dell, S. C. Zimmerman, F.-G. Klärner, *Eur. J. Org. Chem.* **1999**, 2741–2749.
[10] F.-G. Klärner, U. Burkert, M. Kamieth, R. Boese, *J. Phys. Org. Chem.* **2000**, *13*, 604–611.
[11] F. G. Klärner, B. Kahlert, *Acc. Chem. Res.* **2003**, *36*, 919–932.
[12] Both terms—molecular clips and molecular tweezers—are used to describe noncyclic but well preorganized receptor molecules with cavities of flexible size. As noted in M. Harmata, *Acc. Chem. Res.* **2004**, *37*, 862–873, there is no clear-cut structured distinction between tweezers and clips in the literature. We use the two terms to describe the different complex structures of the dimethylene- and trimethylene-bridged clips on the one hand and those of the tetramethylene-bridged tweezers on the other.
[13] M. Kamieth, F.-G. Klärner, F. Diederich, *Angew. Chem.* **1998**, *110*, 3497–3500; *Angew. Chem. Int. Ed.* **1998**, *37*, 3303–3306.
[14] F.-G. Klärner, J. Panitzky, D. Preda, L. T. Scott, *J. Mol. Model.* **2000**, *6*, 318–327.
[15] F. G. Klärner, J. Polkowska, J. Panitzky, U. P. Seelbach, U. Burkert, M. Kamieth, M. Baumann, A. E. Wigger, R. Boese, D. Bläser, *Eur. J. Org. Chem.* **2004**, 1405–1423.
[16] W. Ried, H. Bodem, *Chem. Ber.* **1956**, *89*, 708–712.
[17] 2,3-Bis(dibromomethyl)naphthalene **5** was prepared in a one-step synthesis by photochemically induced NBS bromination of commercially available 2,3-dimethylnaphthalene (Lancaster) in 68% yield.
[18] J. Benkhoff, R. Boese, F.-G. Klärner, *Liebigs Ann.* **1997**, 501–516.
[19] M. P. Cava, D. R. Napier, *J. Am. Chem. Soc.* **1957**, *79*, 1701–1709.
[20] M. P. Cava, R. L. Shirley, *J. Am. Chem. Soc.* **1960**, *82*, 654–656.
[21] M. N. Paddon-Row, H. K. Patney, K. Harish, *Synthesis* **1986**, 328–330.
[22] J. W. Barton, M. K. Shepherd, R. J. Willis, *J. Chem. Soc. Perkin Trans. 1* **1986**, 967–972.
[23] A precedent for the reaction sequence **12c**→**13c**→**1c** is the annellation of a benzene ring to 2,3-dibromonaphthalene described by H. Hart, A. Bashir-Hashemi, J. Luo, M. A. Meador, *Tetrahedron* **1986**, *42*, 1641–1654.
[24] The cleavage of aryl methyl ethers with boron tribromide was reported in J. B. Press, *Synth. Commun.* **1979**, *9*, 407–410.
[25] A nonlinear regression analysis of Equation (3) (Experimental Section) was performed by use of the program TableCurve 5.01, SYSTAT Software Inc., analogous to the computer program HOSTTEST by C. S. Wilcox, N. M. Glagovich, University of Pittsburg, and the program Associate V1.6, B. Peterson, Ph.D. Dissertation, University of California at Los Angeles, 1994.
[26] A. Job, *Ann. Chem.* **1928**, *9*, 113–203.
[27] Titan, v. 1.0.1, Wavefunction Inc., 18401 Von Karman Ave., Ste. 370, Irvine, CA 92612.
[28] M. J. S. Dewar, E. G. Zoebisch, E. F. Healy, J. J. P. Stewart, *J. Am. Chem. Soc.* **1985**, *107*, 3902–3909.
[29] W. J. Hehre, L. Radom, P. von R. Schleyer, J. A. Pople, *Ab Initio Molecular Orbital Theory*, Wiley, New York, **1986**.
[30] A. D. Becke, *J. Chem. Phys.* **1993**, *98*, 5648–5652.
[31] P. C. Hariharan, J. A. Pople, *Chem. Phys. Lett.* **1972**, *16*, 217–219.
[32] An exception seems to be the complexes of **1a** and **1b** with the viologen derivative **19**. In this case complex **19@1a** is found to be more stable than complex **19@1b**. In the structure of complex **19@1a** calculated by a Monte-Carlo conformer search (MacroModel 6.5, AMBER*, 5000 structures)[37,38] the carbonyl oxygen atom of one acetoxy group points toward the pyridinium ring of **19** complexed inside the clip cavity. The resulting attractive O···N^+ interaction may lead to additional stabilization of complex **19@1a**.
[33] T. A. Halgren, *J. Comput. Chem.* **1996**, *17*, 490–519.
[34] S. P. Brown, T. Schaller, U. P. Seelbach, F. Koziol, C. Ochsenfeld, F.-G. Klärner, H. W. Spiess, *Angew. Chem.* **2001**, *113*, 740–743; *Angew. Chem. Int. Ed.* **2001**, *40*, 717–720.
[35] C. Ochsenfeld, F. Koziol, S. P. Brown, T. Schaller, U. P. Seelbach, F.-G. Klärner, *Solid State Nucl. Magn. Reson.* **2002**, *22*, 128–153.
[36] C. Ochsenfeld, J. Kussmann, F. Koziol, *Angew. Chem.* **2004**, *116*, 4585–4589; *Angew. Chem. Int. Ed.* **2004**, *43*, 4485–4489.
[37] F. Mohamadi, N. G. J. Richards, W. C. Guida, R. Liskamp, M. Lipton, C. Caufield, G. Chang, T. Hendrickson, W. C. Still, *J. Comput. Chem.* **1990**, *11*, 440–467.
[38] Macromodel, v. 6.5, Schrödinger, Inc., 1500 SW First Ave., Ste. 1180, Portland, OR 97201.
[39] M. Hesse, H. Meier, B. Zeeh, *Spektroskopische Methoden in der organischen Chemie*, Thieme, Stuttgart, **1991**.
[40] E. M. Kosower, *J. Am. Chem. Soc.* **1958**, *80*, 3253–3260.
[41] E. M. Kosower, M. Mohammad, *J. Am. Chem. Soc.* **1968**, *90*, 3271–3272.
[42] E. M. Kosower, M. Mohammad, *J. Phys. Chem.* **1970**, *74*, 1153–1154.
[43] E. M. Kosower, M. Mohammad, *J. Am. Chem. Soc.* **1971**, *93*, 2713–2719.
[44] C. Reichardt, *Chem. Rev.* **1994**, *94*, 2319–2358.
[45] C. Reichardt, *Solvents and Solvent Effects in Organic Chemistry*, Wiley-VCH, Weinheim, **2003**.
[46] G. Jones II in *Photoinduced Electron Transfer, Part A* (Ed.: M. A. Fox, M. Chanson), Elsevier, Amsterdam, **1992**.
[47] I. Deperasinska, J, Prochorow, J. Dresner, J. Dresner, *J. Lumin.* **1998**, *79*, 65.
[48] H. Gampp, M. Maeder, C. J. Meyer, A. D. Zuberbühler, *Talanta* **1985**, *32*, 257–264.
[49] R. A. Binstead, "SPECFIT", Spectrum Software Associates, Chapel Hill, NC, **1996**.

Received: December 7, 2004
Published online: March 30, 2005